EUROPEAN ORGANIZATION FOR NUCLEAR RESEARCH

CERN-EP/89-180
December 22th, 1989

EXPERIMENTAL RESULTS ON PROTON DIFFRACTIVE DISSOCIATION -- STUDY OF THE QUARK-DIQUARK POMERON COUPLING

M. Asai[7d], J.L. Bailly[9], H. Böttcher[13], F. Bruyant[3], C. Caso[5], Y. Chiba[7d], H. Dibon[12], B. Epp[6], A. Ferrando[8], F. Fontanelli[5], S.N. Ganguli[1], T. Gémesy[2], R. Hamatsu[7a], P. Hidas[2], T. Hirose[7a], J. Hrubec[12], T. Kageya[7a], N. Khalatyan[11], E. Kistenev[11], I. Kita[7b], S. Kitamura[7a], V. Kubik[11], J. MacNaughton[12], M. Markytan[12], S. Matsumoto[7c], I.S. Mittra[4], L. Montanet[3], G. Neuhofer[3], G. Pinter[2], P. Porth[12], T. Rodrigo[8], J. Singh[4], S. Squarcia[5], K. Takahashi[7b], R. Tanaka[7c], L.A. Tikhonova[10], U. Trevisan[5], R. Wischnewski[13], T. Yamagata[7a], S.A. Zotkin[10]

NA23, EHS-RCBC Collaboration

1 Tata Institute of Fundamental Research, 400005 Bombay, India.
2 Central Research Institute for Physics, H-1525 Budapest 114, Hungary*).
3 CERN, European Organization for Nuclear Research, CH-1211 Geneva 23, Switzerland.
4 Panjab University, 160014 Chandigarh, India.
5 University of Genova and INFN, I-16146 Genova, Italy.
6 Institut für Experimentalphysik, A-6020 Innsbruck, Austria**).
7a Tokyo Metropolitan University, Tokyo 158, Japan.
7b Tokyo University of Agriculture and Technology, Tokyo 184, Japan.
7c Chuo University, Tokyo 112, Japan.
7d Hiroshima University, Hiroshima 730, Japan.
8 Centro de Investigaciones Energéticas, Medioambientales y tecnológicas, E-28040 Madrid, Spain.
9 Université de l'Etat, Faculté des Sciences, B-7000 Mons, Belgium.
10 Moscow State University, SU-117234 Moscow, USSR.
11 Institute for High Energy Physics, Serpukhov, SU-142284 Protvino, USSR.
12 Institut für Hochenergiephysik, A-1050 Wien, Austria**).
13 Institut für Hochenergiephysik, Akad. der Wissensch., 1615 Zeuthen, DDR.

*) Supported by the Hungarian Science Research Foundation.
**) Supported in part by the Fonds zur Förderung der Wissenschaftlichen Forschung.

(To be submitted to Zeit. Physics C)

ABSTRACT

Properties of proton diffractive dissociation have been investigated for four-prong final states in proton-proton reactions at 360 GeV/c, in particular for $pp \rightarrow pp\pi^+\pi^- m\pi^o$ (m = 0,1,2). Mass distributions and decay angular distributions are given. The decay of the diffractive system is seen to be very anisotropic, and large p_T is suppressed at higher masses. It is found that the "Pomeron" couples with a single valence quark of the incident proton, but indications for a diquark-Pomeron coupling are also found. Similarities with fragmentation in lepton-hadron deep inelastic scattering are underlined.

1. INTRODUCTION

Single diffractive dissociation (SDD) plays an important role in hadron-hadron interactions at low transverse momentum and high energies. This process may be described in terms of the exchange of a "Pomeron", a hypothetical entity with the quantum numbers of the vacuum carrying only energy and momentum [1]. In single diffraction, the Pomeron is absorbed by only one of the initial state particles leading to an intermediate excited state of mass M_X which subsequently fragments. It has been pointed out that the Pomeron may create a quark-antiquark pair which couples with the valence quarks resulting in multi-quark diffractive states [2].

For invariant masses of the intermediate excited state (M_X) near threshold, resonances have been found to play a prominent role. However, at incident energies of several hundred GeV, an excited state well above threshold (e.g. > 3 GeV) can be easily produced. Such "high mass" diffractive dissociation is a typical example of a peripheral collision at high energies. This process cannot be calculated using perturbative quantum chromodynamics (QCD); nevertheless it is of much interest since it contributes significantly to the total cross-section in proton-proton and proton-antiproton scattering [3].

Single diffractive dissociation has been studied for various incident particles from low energies to the highest available energies at the SPS Collider [4] and is characterized by scaling of the invariant cross-section in terms of the variables M^2_X/s and of the four-momentum transfer squared, t [5].

Although many experiments have studied diffractive dissociation, there is very little experimental information concerning the internal structure of the excited system. Such information may shed light on the nature of the Pomeron [6-14]. Historically it has been proposed that the diffractively excited system may decay isotropically [8,9] or alternatively elongated along the longitudinal direction [10]. Recently this question has been investigated again in several experiments [6,11-14]. This is also done in the present paper on the basis of angular and Feynman-x distributions. One possible interaction mechanism for this process is that the Pomeron couples in a pointlike fashion to a quark in the proton similarly to a photon in deep inelastic lepton-hadron scattering [15]. The Pomeron can also couple to gluons in the proton [16].

In this paper, we shall investigate experimentally certain characteristic features of "high mass" diffractive dissociation, confining our attention to quark-diquark fragmentation of the excited intermediate state produced by the Pomeron single quark (diquark) coupling.

Figure 1a shows a schematic diagram for beam diffractive dissociation. In the Gottfried-Jackson frame, the rest frame of the excited system composed of the Pomeron and of the incident proton, these two particles collide head-on as shown in Fig. 1b.

The experimental procedure and the details of the method used for selecting a diffractive component are given in Section 2. Experimental results are presented in Section 3 and compared with models in Section 4. Conclusions are given in Section 5.

2. EXPERIMENTAL PROCEDURE

The NA23 experiment was performed at the CERN SPS with the European Hybrid Spectrometer (EHS). It consisted of a Rapid Cycling Bubble Chamber (RCBC), combined with upstream and downstream spectrometers. The downstream spectrometer included wire and drift chambers to complement the momentum information for charged tracks obtained from RCBC, a pictorial drift chamber (ISIS) giving particle identification information based on relativistic rise of ionization and two gamma detectors allowing the reconstruction of π^o's produced in the forward hemisphere.

Details about detectors, trigger efficiency, data handling, particle identification and π^o reconstruction have been published elsewhere [17-20]. The interaction trigger used for on-line data acquisition has a global efficiency of 97% for the "four-prong" topologies which will be used in this paper [18]. However, this efficiency strongly depends on the configuration of the four prongs, being low for "target" diffraction and, on the contrary, large for "beam" diffraction. The interaction trigger was designed to discriminate between non-interacting beam particles and elastic and target diffraction dissociation events with fast forward going particles produced with small momentum transfers. The incident beam had approximately a rectangular cross-section at the level of the vertex detector (RCBC), with a horizontal width of 3.5 mm (FWHM) and a vertical extension of ~ 5 cm; the trigger hodoscopes had a horizontal-vertical asymmetry which resulted in a loss of elastic and single diffraction events with a fast forward going particle at $\theta = \pm 90^o$, θ measuring the azimuthal angle. The experimental distribution of θ, which should be flat, showed that we lose less than 4% of the beam fragmentation events, whereas 25% of the target fragmentation are lost . In the following, we shall restrict to the analysis of the beam fragmentation events, for which the trigger biases are minimal. Furthermore, most of the azimuthal losses affect small momentum transfers, i.e. small masses M_X for the intermediate excited state. A cut on M_X will eliminate any residual bias due to the interaction trigger.

Single diffraction interactions lead to relatively simple topologies as compared with other interactions. We have limited our analysis to a sample of "four-prong events" since, for this

sample, single diffraction is easy to identify and the trigger losses are minimal (at least for beam diffraction).

The sample consists of 2822 four-prong events without strange particle decays.

The reactions relevant for the present analysis are therefore:

$pp \rightarrow pp\pi^+\pi^- + m\pi^o$, where m = 0,1,2	(4C fit)	(1)
$pp \rightarrow pp\pi^+\pi^-\pi^o$	(1C fit)	(2)
$pp \rightarrow p\pi^+\pi^+\pi^-n$	(1C fit)	(3)
$pp \rightarrow p\pi^+\pi^+\pi^-$ + multi-neutrals	(no fit)	(4)

In reaction (1), the π^o are reconstructed using the gamma detector information. In reaction (2) and (3), the π^o and neutron, respectively, are undetected. Reaction (4) corresponds to interactions where two neutrals, at least, are undetected.

Particle identification, which allowed the separation of protons from π^+, for charged positive tracks, was used in the following way: based on the information measured in ISIS [19], a χ^2 probability was computed for each mass assignment. A hypothesis was rejected if its probability was less than 1%.

46% of the four-prong sample, i.e. 1289 events, give no-fit (reaction 4) whereas 1371 events yield at least one kinematic fit with a χ^2 probability larger than 1%. Moreover, for events with more than one acceptable kinematic fit, particle identification was used to select the most probable hypothesis. In this way, we were able to establish a one-to-one correspondence between each event and one of the reactions (1-4).

The sample of single diffraction dissociation was then defined in the following way:

- Each identified proton with Feynman x (x_F), i.e. with a fractional longitudinal momentum larger than $|x_F| = 0.85$, is designated "spectator". This value was chosen since in a previous work [21], it was shown that this selection is very efficient to isolate single diffraction, keeping however a background of other inelastic interactions of the order of 15% at our energy. This selection is also justified by optical model considerations [5].

- The rapidity gap Δy between the "spectator" proton and the nearest neighbouring charged particle must be larger than 2.0. We first intuitively justify this choice by showing in Fig. 2a the average value of the relative excited mass ($\langle M_X^2/s \rangle$) for interactions with a "spectator" proton

and for various values of the rapidity gap Δy: above $\Delta y = 1$, the distribution falls quickly as Δy increases, as it should for "central" inelastic interactions. The tendency is reversed for small values of $<M_X^2/s>$, with the distribution having an inflection point at $\Delta y \sim 2$. This is taken as an indication of a transition between two distinct mechanisms.

Another indication that $\Delta y \sim 2$ corresponds to a transition between two distinct mechanisms is provided by Fig. 2b where the number of events which are kept after successive Δy cuts show again a change of trend around $\Delta y \sim 2$.

Of the 1371 events satisfying the kinematic conditions corresponding to reaction (1-3), 629 had one positive particle fulfilling the condition: $x < -0.85$. 544 of those also satisfied the criterion: $\Delta y > 2.0$. Finally, 498 good candidates for "beam single diffraction" (BSD) were found with a well-identified spectator proton. To this sample of BSD one may add 105 candidates extracted from reaction (4) once the x_F and Δy cuts are applied.

Among the 498 BSD events with a well-defined kinematic fit (reactions 1-3) one finds: 229 "4C fits" which correspond to reaction (1) with 0, 1, or $2\pi^o$ (167, 45 and 17 events, respectively). For this sample, the number of "low mass" BSD ($M_X < 2.8$ GeV) and "high mass" ones were 130 and 99, respectively.

3. EXPERIMENTAL RESULTS

Figure 3 shows the distribution of M_X, the mass of the excited intermediate state produced in BSD. M_X was defined as the effective mass of the final state, excluding the spectator proton, for reactions (1)-(3). In the case of multi-neutral undetected final states [reaction (4)], the missing mass to the spectator proton was used.

One observes in Fig. 3b the well-known $1/M_X^2$ linear dependence [5], for "high" mass values of M_X, i.e. above ~ 3 GeV. In the Regge picture, this arises from triple Pomeron dominance [22]. A fit of the form

$$\ln N = a + b \ln (1/M_X^2)$$

yields $a = 6.52 \pm 0.02$ and $b = 0.94 \pm 0.02$ above $M_X = 2.8$ GeV. In the following, the events with $M_X > 2.8$ GeV will be referred to as "high mass diffractive dissociation events".

The M_X distributions for the 4C fit interactions [reaction (1)] with 0,1 or 2 associated π^o are shown in Figs, 4a-c, respectively. One notices that the average value of M_X increases as the multiplicity increases in the final state.

Figure 5 shows the Feynman x distributions for positive, negative and neutral particles produced in the selected BSD sample. The isolated positive particle distribution at $x_F < -0.85$ corresponds, of course, to the "spectator" protons. One notices that all three charges (positive, negative, neutral particles) follow the same trend for $x \sim 0\text{-}0.2$ but that positive particles depart from this common trend as x_F increases, the large x_F values being mainly populated by positive particles.

Figure 6 shows the average $|p_L|$ and p_T, the longitudinal and transversal momenta, respectively, of the secondary particles for the BSD sample, as a function of M_X. One notices a striking difference in the behaviour of these distributions, the longitudinal component showing a continuous rise with increasing M_X whereas the transverse component tends to flatten at 0.4-0.5 GeV. This behaviour is similar to the one observed for hadrons produced in e^+e^- annihilations into quark jets (the longitudinal and transverse momenta being then defined with respect to the "jet axis"). The average values of p_T for protons, charged pions and neutral pions are given in Table 1, for $M_X < 2.8$ GeV and $M_X > 2.8$ GeV. The results are given for the BSD sample of reaction (1) (4C fit events) but the values obtained for reactions (2) and (3) are not significantly different.

To look for further dynamical structures, we studied the properties of the diffractive system in terms of the Gottfried-Jackson angle θ, where θ is the angle between the incident proton and decay particle in the rest frame of the diffractive system. To define the Feynman x in this system we projected the momenta onto the direction of the incident proton in this frame (Fig. 1b).

The analysis described in the following uses only the 4C fit events (reaction 1) with a "high mass" excited diffractive system ($M_X > 2.8$ GeV).

Figure 7 shows the Gottfried-Jackson angular distributions for the π^+, the π^-, and the protons of the "high mass" BSD sample, as well as the corresponding Feynman x distribution.

The protons exhibit a pronounced peak in the forward direction ($\cos\theta = +1$) which is balanced by a backward accumulation for π^- (Fig. 7b) also for π^0 (not shown). The π^+, on the other hand, do not show a significant forward-backward asymmetry, but still exhibit a large anisotropy.

Obviously, these angular distributions exclude the possibility of an isotropic decay of the excited system: they confirm the high p_T suppression observed for single diffraction at ISR energies [11]. A comparison of the angular distributions for events with M_X below or above 2.8

GeV shows that this anisotropy is larger for higher masses (A = 5.06 for $M_X > 2.8$ GeV as opposed to A = 2.0 for $M_X < 2.8$ GeV. A is the ratio of the number of particles with $|\cos\theta| > 0.5/|\cos\theta| < 0.5$).

A non-negligible fraction of protons is however going backward and produces a secondary peak at $\cos\theta = -1$ (or $x_F = -1$) (Fig. 7c,f). In view of the particular interest of this observation, the events containing backward going protons were scrutinized one by one, and were all found to correspond effectively to a non-ambiguous 4C fit hypothesis leading to the "abnormal" emission of a backward proton (compensated by a forward π^+ emission). A hypothetical double Pomeron exchange is completely negligible at the present incident momentum and at the sensitivity of this experiment. Moreover, it was checked that none of the events containing a backward proton could be attributed to double-Pomeron exchange. Λ^o decaying close to the primary vertex were also excluded.

A natural interpretation of these observations can be attempted in terms of a dominant Pomeron-valence quark collision complemented by a significant Pomeron-valence diquark interaction. Similar phenomena were observed in deep inelastic muon-proton [23] scattering.

The flavour composition of forward or backward going diquark can be approximately estimated by the charge state of the pion going in the opposite direction. The diquark composition can be (ud) if a positive pion ($u\bar{d}$), [or (uu) if a negative pion ($\bar{u}d$)] is going in the opposite direction. The dependence of the (uu)/(ud) ratio on the proton direction is shown in Table 2 for $M_X < 2.8$ GeV and $M_X > 2.8$ GeV. Whereas one does not observe a dependence of (uu/ud) on the direction of the final state proton for "low masses" M_X, this ratio is strongly direction dependent for $M_X > 2.8$ GeV.

Figure 8 shows strong angular correlations between the proton, the π^+ and π^- in the decay of the "high mass" diffractive system.

4. COMPARISON WITH MODELS

We have compared our experimental data with Monte Carlo generated events, using the Lund Models FRITIOF [24] and PYTHIA [25]. Since we could not find significant differences between the two models, we shall, in the following, limit the comparison of the experimental data to PYTHIA (we have used the version 4.8 of PYTHIA).

PYTHIA treats hadron-hadron interactions in terms of the parton-parton picture, including an attempt to describe single diffraction with a Pomeron-quark interaction. The Monte-Carlo events were submitted to the same selection criteria as those applied to real events. A

fragmentation model has a hard task, in general, to reproduce the few body final states because the fragmentation chain has to stop after very few iterations and four-momentum conservation strongly influences the final hadron state. One should also add that the PYTHIA sample can only be regarded as a first approximation to the real single diffractive process since in PYTHIA the 1/2 isospin baryon resonances are not included and we know that these resonances play an important role in diffractive dissociation. Another shortcoming of the model may also come from the simplified treatment of the decay angular distributions of resonances.

The predictions of PYTHIA are shown in Fig. 7: the general trends are in global agreement with the experimental data. One notes, however, striking differences: the π^+ and π^- distributions, which are identical according to PYTHIA, show experimentally significant differences. For the proton distributions, PYTHIA fails to reproduce the backward peak, clearly visible in both $\cos\theta$ and x_F distributions.

To explain the differences observed between the model predictions and the data, one may invoke, as already mentioned in Section 3, a Pomeron-diquark scattering and/or the presence of baryon resonances in the final state, which may interfere and conspire to produce some of the structures observed in these angular distributions.

5. CONCLUSIONS

Using data obtained on proton-proton interactions at 360 GeV, we have investigated the properties of particle production for "high mass" beam diffraction dissociation (BSD) mainly in the topologies $pp \rightarrow pX$, where $X = p\pi^+\pi^- m\pi^0$ ($m = 0,1,2$).

For the 4C fit "high mass" BSD sample, we have carried out an analysis in the Gottfried-Jackson frame. We have observed that the "decay" of the diffractive system is very anisotropic, and that larger p_T are suppressed.

We have presented evidence that the particle exchanged in the BSD process, presumably the Pomeron, collides with a single valence quark (or diquark) in the incident proton. This collision causes a quark-diquark dissociation of the incident proton which is reflected in the kinematic behaviour of the secondary particles due to hadronization of the quark and diquark. These results are in accord with the idea that the Pomeron couples in a point-like way to a single quark and diquark of the target hadron and the struck quark or diquark undergoes a significant scattering, whereas the spectator diquark or single quark goes forward. The trend observed for the (uu)/(ud) ratio, which is far from the values predicted by exact SU(6), could confirm the SU(6) symmetry breaking observed in other experiments [26].

The Pomeron in this case is very similar to gauge bosons in deep inelastic lepton-hadron scattering [24]. The agreement of the Feynman x distributions for "high mass" BSD in proton-proton scattering with those for antineutrino-proton deep inelastic scattering (Fig. 9) indicates that once the quark-diquark pair is created the hadronization process of this pair proceeds in a quite universal way independently of any details of the initial interactions.

REFERENCES

[1] M.L. Good and W.D. Walker, Phys. Rev. 120 (1960) 1857.

[2] V. Innocente et al., Phys. Lett. B169 (1986) 285.
J. Ranft, Z. Phys. C 33 (1987) 517.
T. Hirose et al., Preprint TMU-HEL 8407 (1984).

[3] Y. Hattori et al., Journal of the Phys. Soc. Japan 51 (1982) 3761.
J.D. Bjorken, Proc. Int. Symp. on Physics of Proton-Antiproton Collisions, Tsukuba (1985), 520 (eds. Y. Shimisu and K. Takikawa), KEK 85-5.
J.. Timmermans, ibid 46.

[4] M. Bozzo et al., Phys. Lett. 136B (1984) 217.

[5] S.P. Misra et al., Phys. Rev. D 22 (1980) 1574.
K. Goulianos, Phys. Rep. 101 (1983) 169.

[6] R608 Collaboration, A.M. Smith et al., Phys. Lett. 163B (1985) 267.
A.M. Smith et al., Phys. Lett. 167B (1986) 248.

[7] For example, see
F.E. Low, Phys. Rev. D 12 (1975) 163.
S. Nussinov, Phys. Rev. Lett 34 (1975) 1286, and Phys. Rev. D 14 (1976) 246.
G. Ingelman and P.E. Schlein, Phys. Lett. 152B (1985) 256.

[8] R. Hwa, Phys. Rev. Lett. 26 (1971) 1143.

[9] M. Jacob and R. Slansky, Phys. Rev. D 5 (1972) 1847.

[10] D. Amati, A. Stanghellini, and S. Fubini, Nuovo Cimento 26 (1962) 896.

[11] A. Breakstone et al., Z. Phys. C 40 (1988) 207.

[12] D. Bernard et al., Phys. Lett. 166B (1986) 459.

[13] R.E. Ansorge et al., Z. Phys. C 33 (1986) 175.

[14] M. Adamus et al., Z. Phys. C 39 (1988) 301.

[15] A. Donnachie et al., Nucl. Phys. B 244 (1984) 322.

[16] P. Chauvat et al., Phys. Lett. 148B (1984) 382.

[17] M. Aguilar-Benitez et al., Nucl. Instrum. Methods A 205 (1983) 79, and Nucl. Instrum. Methods A 258 (1987) 26.

[18] J.L. Bailly et al., Z. Phys. C 23 (1984) 205.

[19] W.W.M. Allison et al., Nucl. Instrum. Methods 119 (1974) 499, and ibid 163 (1979) 331.

[20] J.L. Bailly et al., Z. Phys. C 22 (1984) 119.

[21] M. Asai et al., Z. Phys. C 27 (1985) 11.

[22] D.P. Roy and R.G. Roberts, Nucl. Phys. B 77 (1974) 240.
R.D. Field and G.C. Fox, Nucl. Phys. B 80 (1974) 367.

[23] M. Arneodo et al., Phys. Lett. 150B (1985) 458.

[24] B. Andersson et al., Phys. Rep. 97 (1983) 31.

[25] H.U. Bengtsson and T. Sjöstrand, Lund LUTP 87-3.

[26] Z. Dziembowski et al., Z. Phys. C 10 (1981) 231.

[27] M. Derrick et al., Phys. Rev. D 24 (1981) 1071.

Table 1

Average transverse momentum: $\langle p_T \rangle$ (GeV) for protons, $\pi^{\pm}$ and π^{o} produced in the excited diffractive system from the BSD sample of reaction (1).

	$M_X > 2.8$ GeV	$M_X < 2.8$ GeV
p	0.50 ± 0.03	0.37 ± 0.02
$\pi^{\pm}$	0.46 ± 0.02	0.27 ± 0.01
π^{o}	0.30 ± 0.03	0.31 ± 0.04

Table 2

(uu/ud) ratio of the diquark which participates (proton going backward) or not (proton going forward) in the Pomeron-hadron collision

	$M_X > 2.8$ GeV	$M_X < 2.8$ GeV
Proton backward	0.17 ± 0.10	1.1 ± 0.4
Proton forward	1.1 ± 0.3	1.1 ± 0.2

Figure captions

Fig. 1 a) Schematic diagram for beam diffractive dissociation. b) Schematic diagram of Pomeron-proton scattering in the Gottfried-Jackson frame. The invariant mass of the system is denoted by M_X and the direction of the incident proton (dashed line in the figure) is chosen as $\theta = 0$.

Fig. 2 a) $<M_X^2/s>$ distribution as function of Δy. b) Variation of the number of events selected as function of Δy.

Fig. 3 Invariant mass, M_X, distribution. a) Linear scale: the shaded area shows the $p\pi^+\pi^-$ effective mass in the case of reaction (1). b) Logarithmic scales. The dashed line is proportional to $1/M^2_X$.

Fig. 4 Effective mass distributions for different multiplicities in the final state: a) $M_X = M(p\pi^+\pi^-)$, b) $M_X = M(p\pi^+\pi^-\pi^o)$, and c) $M_X = M(p\pi^+\pi^-\pi^o\pi^o)$.

Fig. 5 Feynman-x distribution of secondary particles in the c.m. system separated according to their charge.

Fig. 6 Average of the transverse and longitudinal momenta (circles and crosses, respectively) as functions of the mass of the excited system, M_X.

Fig. 7 Gottfried-Jackson angular distributions and Feynman-x distributions for: π^+ (a,d), π^- (b,e), and p (c,f) of the "high mass" BSD events, reaction (1). The curves represent the distributions obtained by Monte Carlo generation using PYTHIA.

Fig. 8 Scatter plot of $\cos\theta_{\pi^\pm}$ versus $\cos\theta_p$ for reactions (1) and (2).

Fig. 9 Feynman-x distribution in the Gottfried-Jackson frame. Dashed histogram shows data for negative hadrons in antineutrino-proton deep inelastic scattering [24], and the solid line histogram shows negative pions of our proton-proton "high mass" BSD sample.

a)

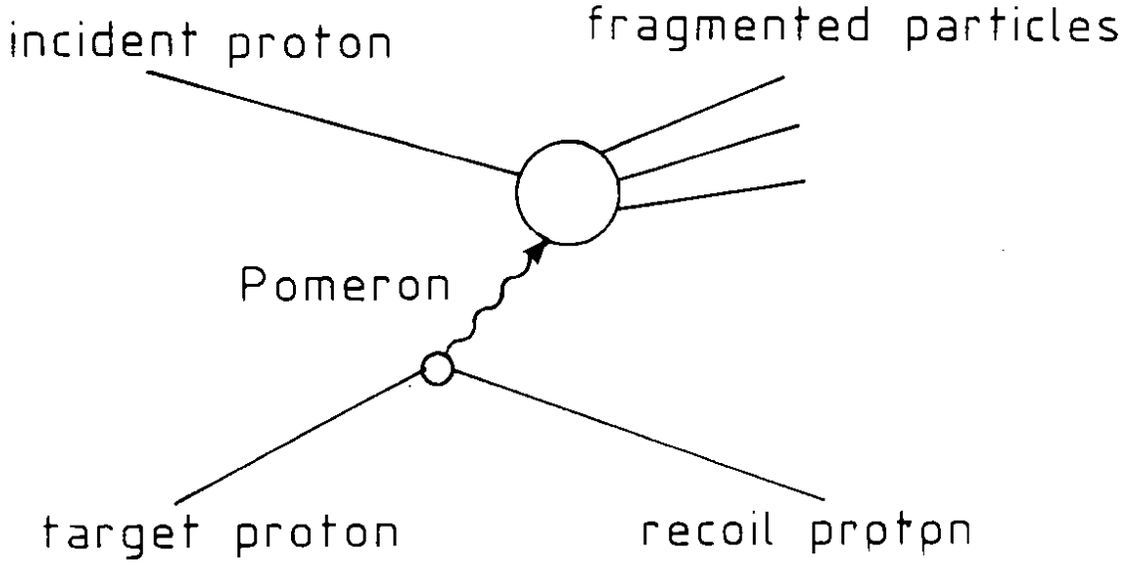
incident proton
fragmented particles
Pomeron
target proton
recoil proton

b)

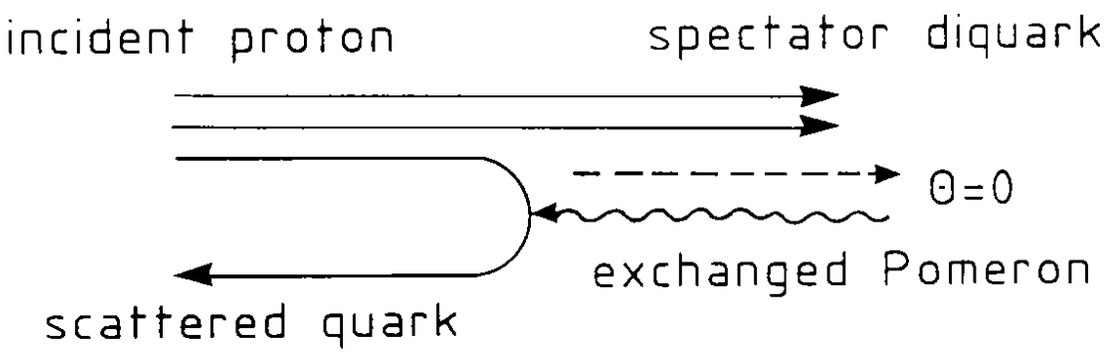
incident proton
spectator diquark
θ=0
exchanged Pomeron
scattered quark

Fig. 1

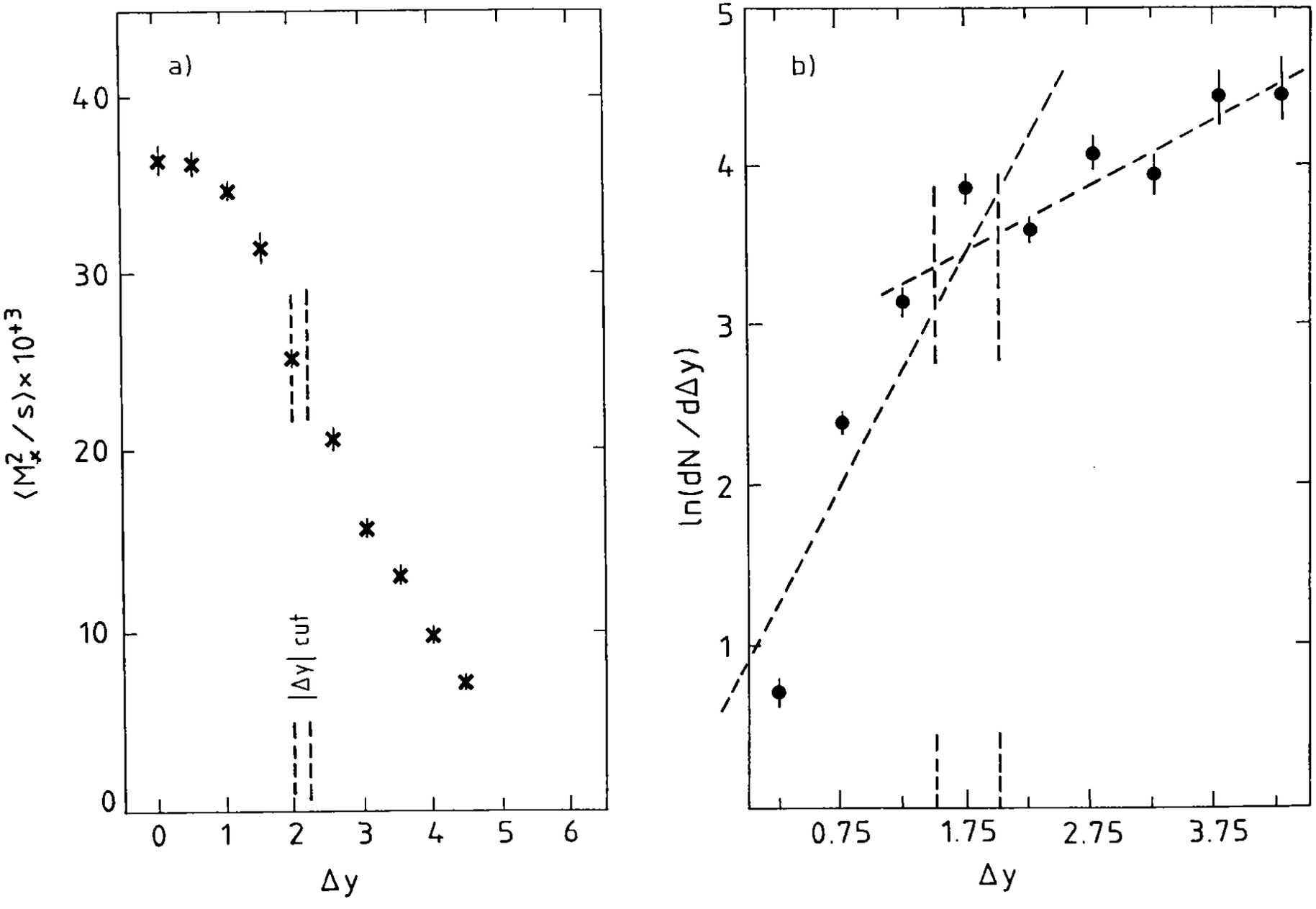
a)
b)
$\langle M_x^2 / s \rangle \times 10^{+3}$
$\ln(dN / d\Delta y)$
Δy
Δy
$|\Delta y|$ cut
0
10
20
30
40
1
2
3
4
5
0
1
2
3
4
5
6
0.75
1.75
2.75
3.75

Fig. 2

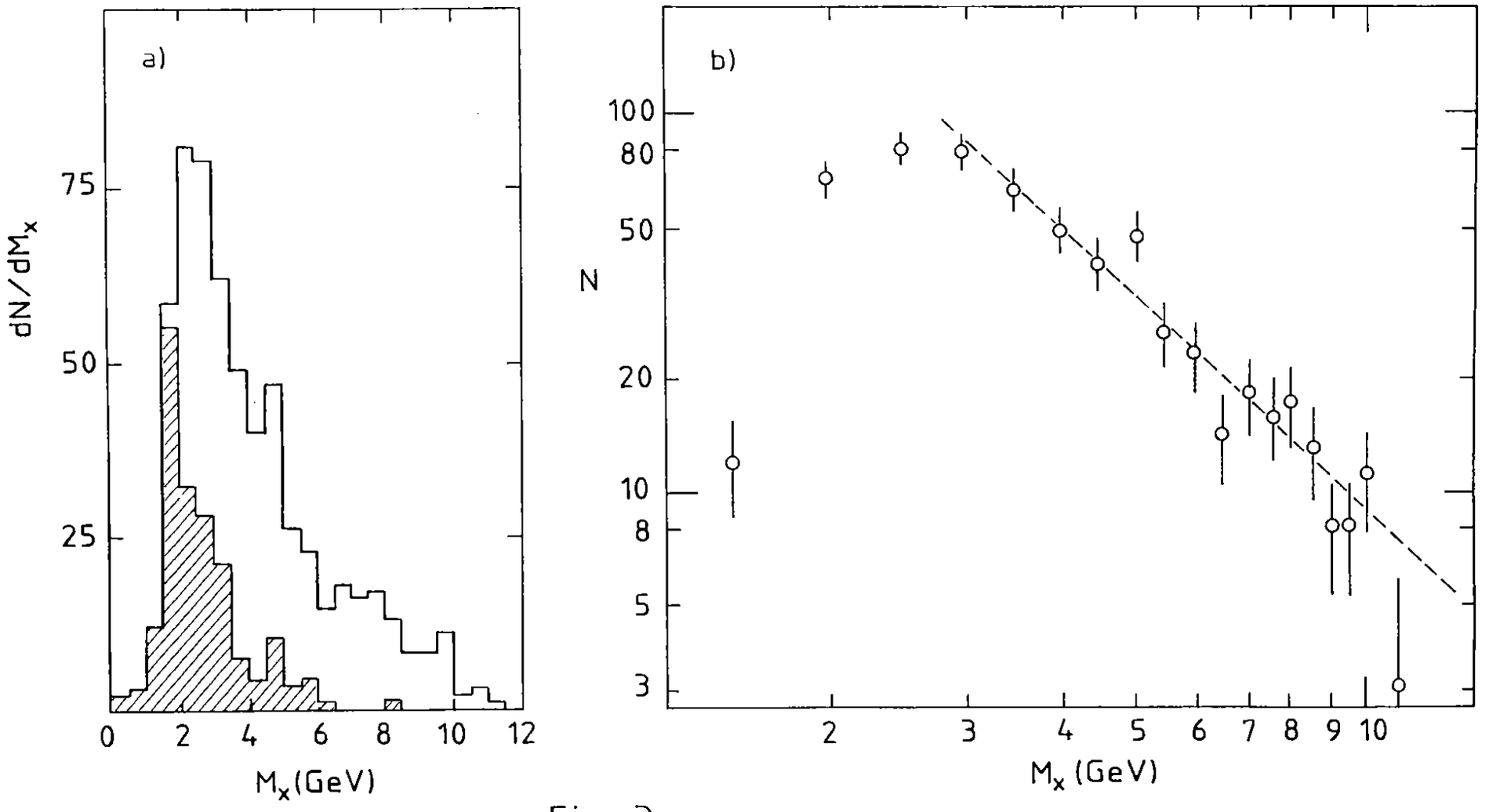
a)
dN/dM$_x$
75
50
25
0
2
4
6
8
10
12
M$_x$(GeV)
b)
N
100
80
50
20
10
8
5
3
2
3
4
5
6
7
8
9
10
M$_x$ (GeV)

Fig. 3

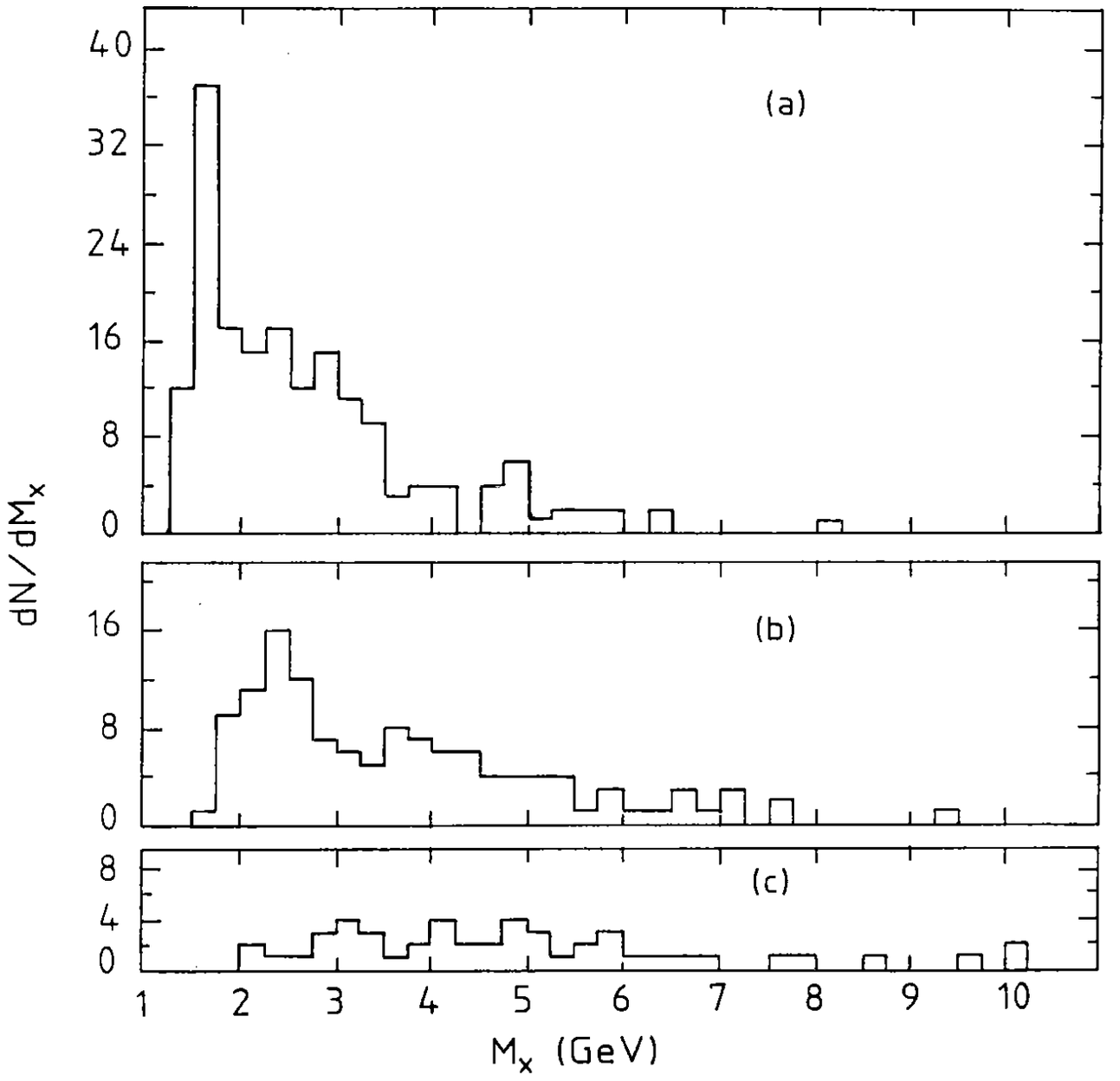

Fig. 4

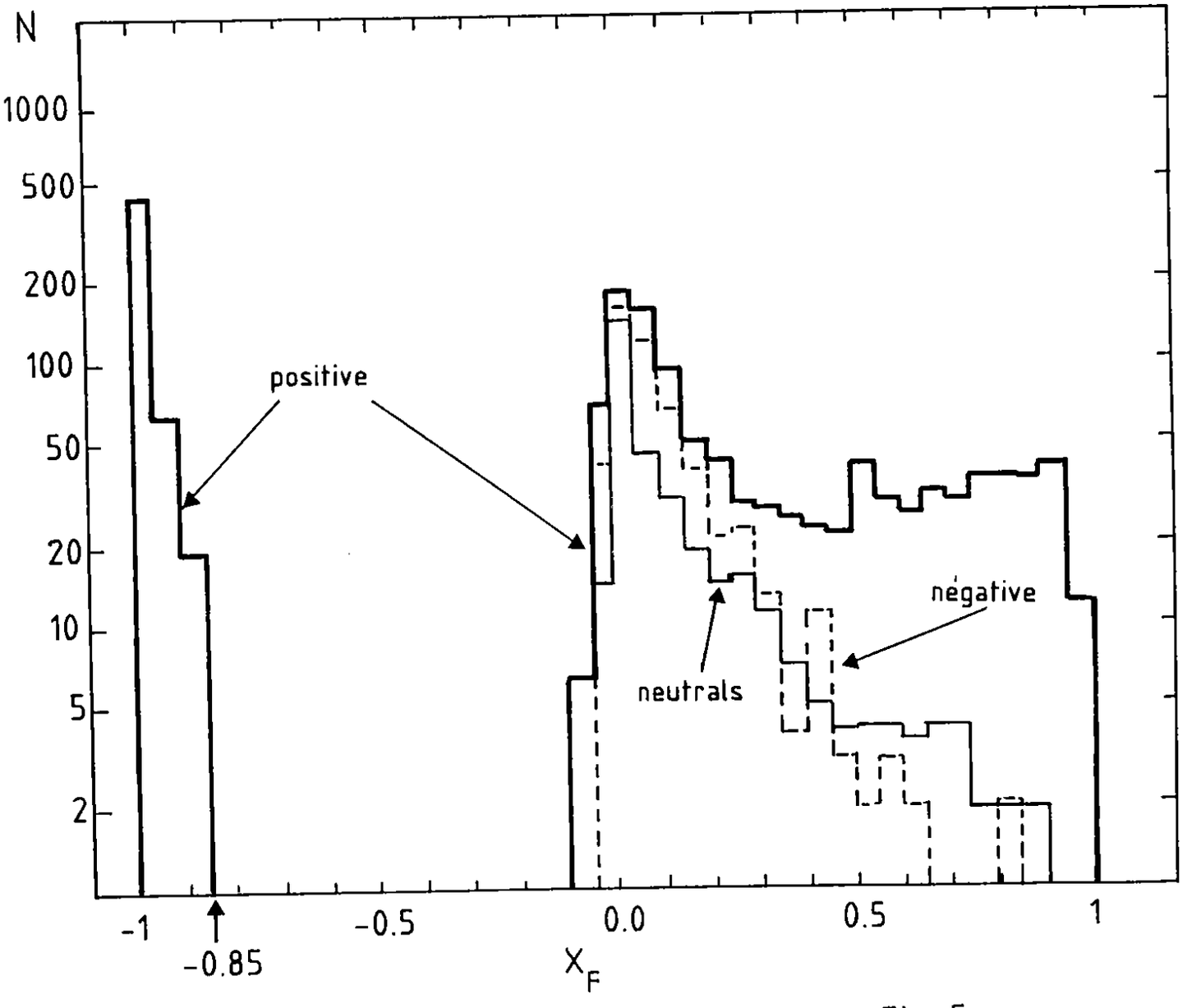
N
1000
500
200
100
50
20
10
5
2
positive
négative
neutrals
-1
-0.85
-0.5
0.0
0.5
1
X_F

Fig. 5

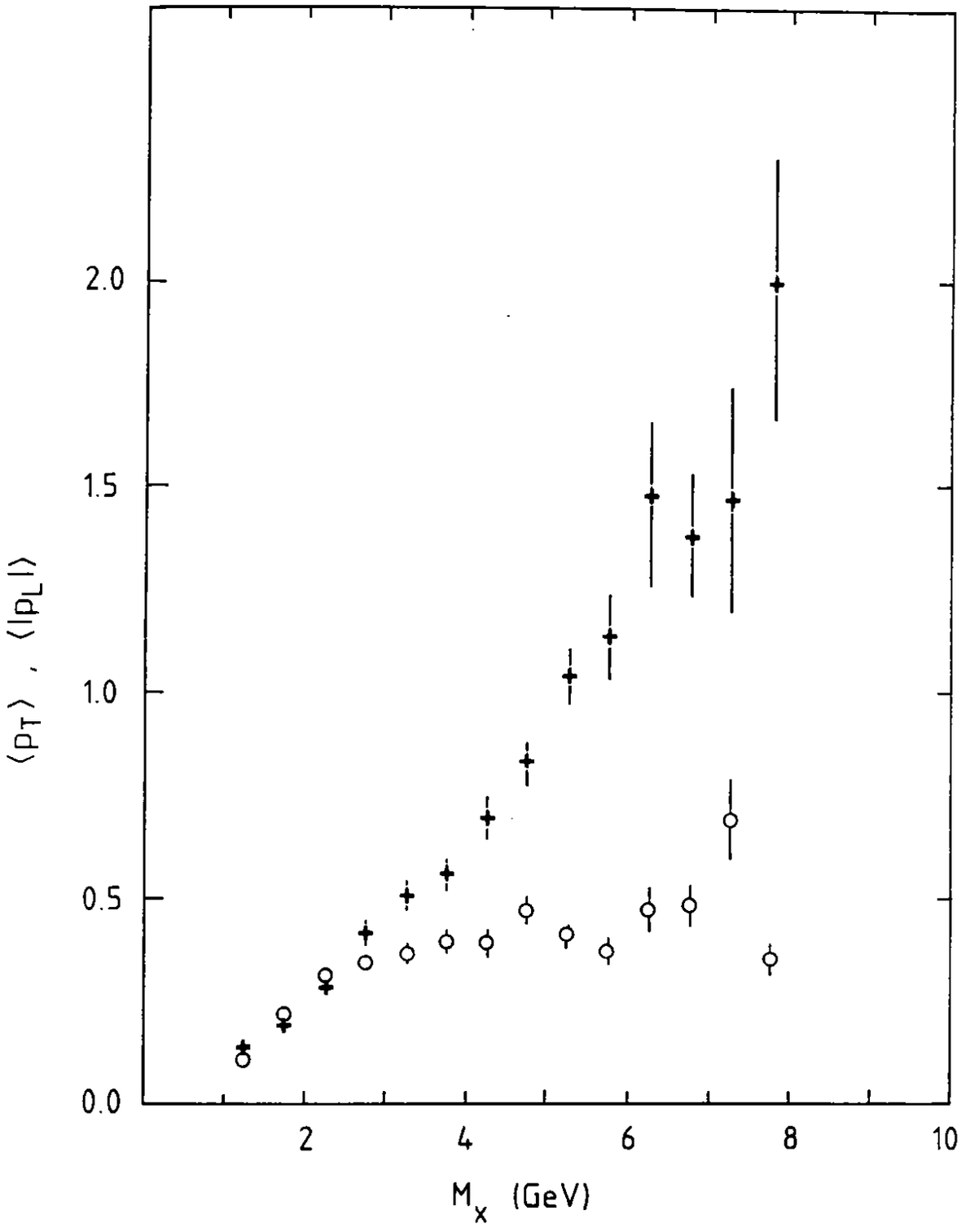

Fig. 6

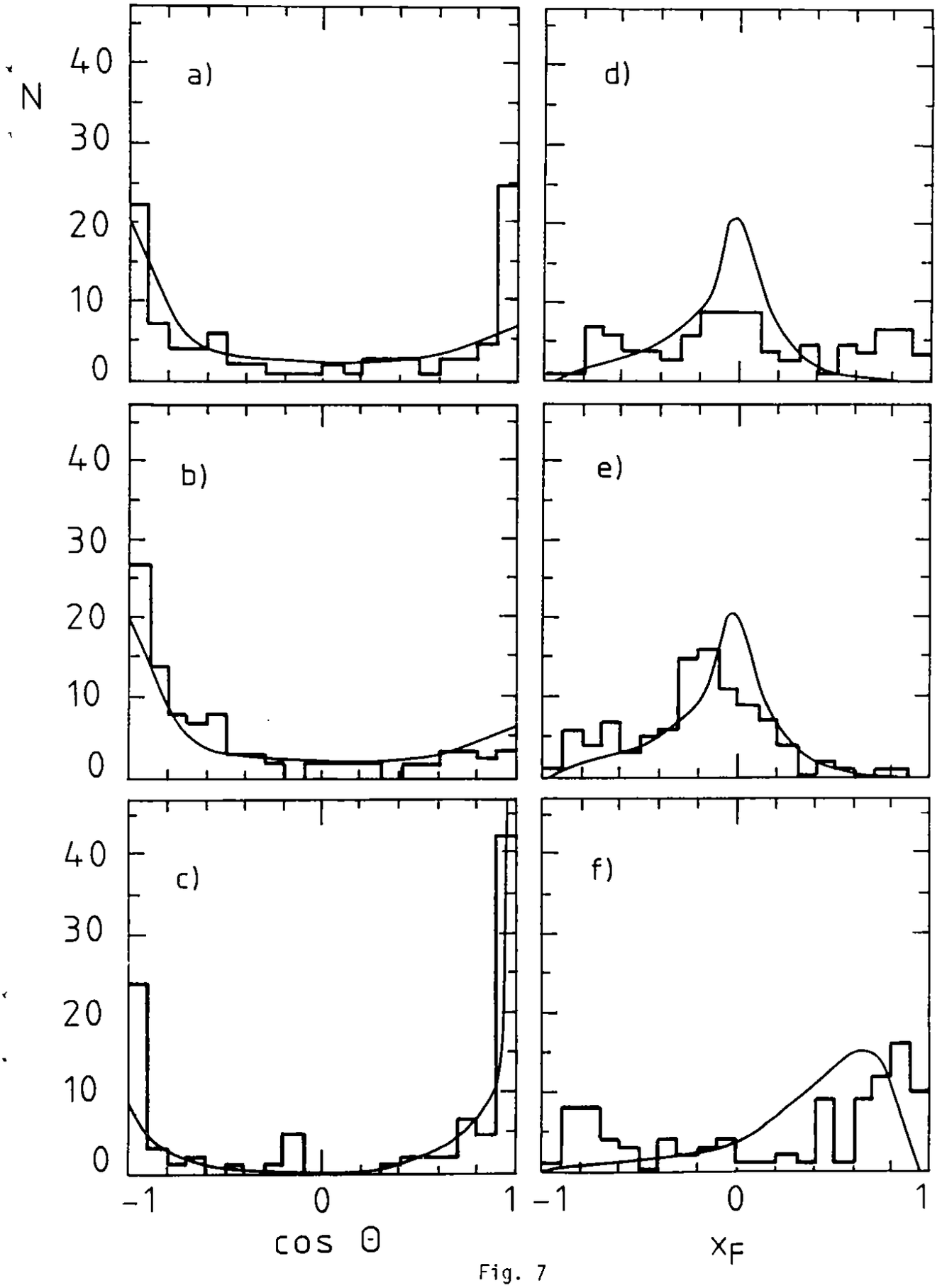

Fig. 7

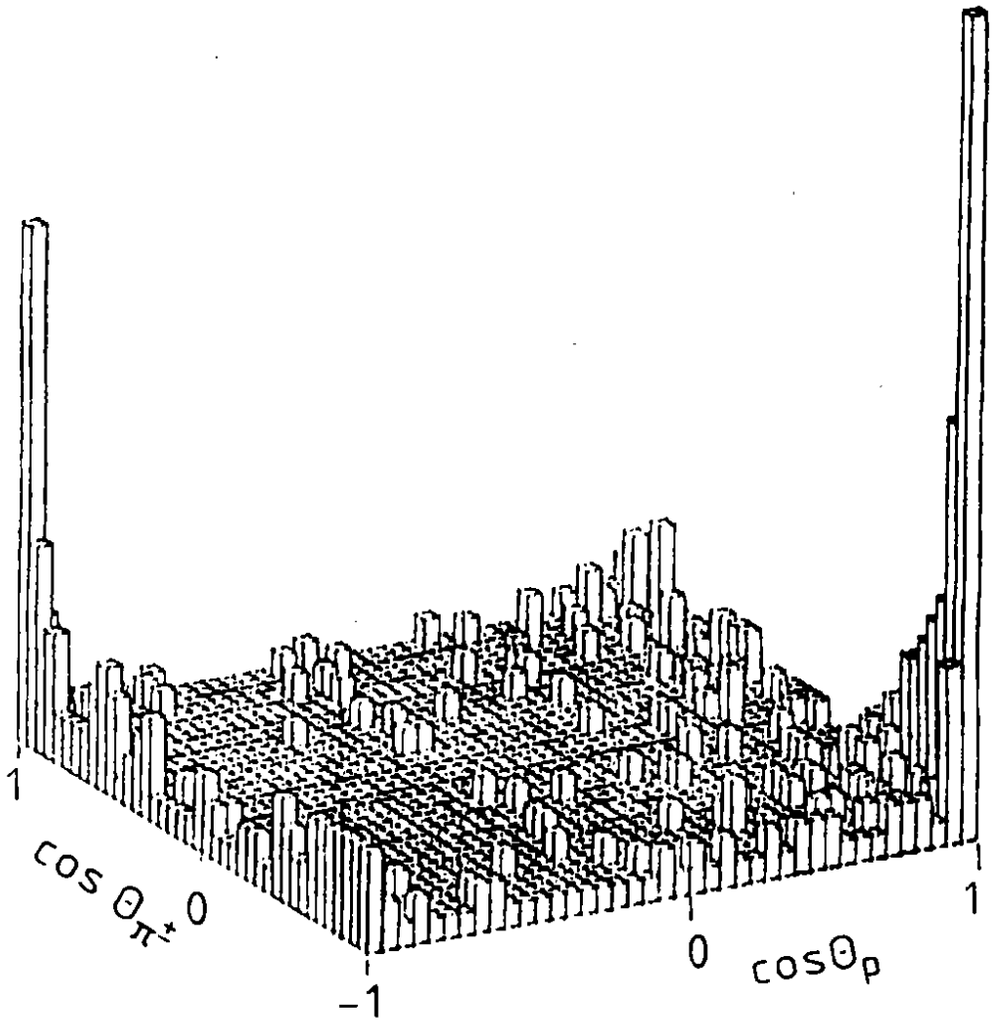

Fig. 8

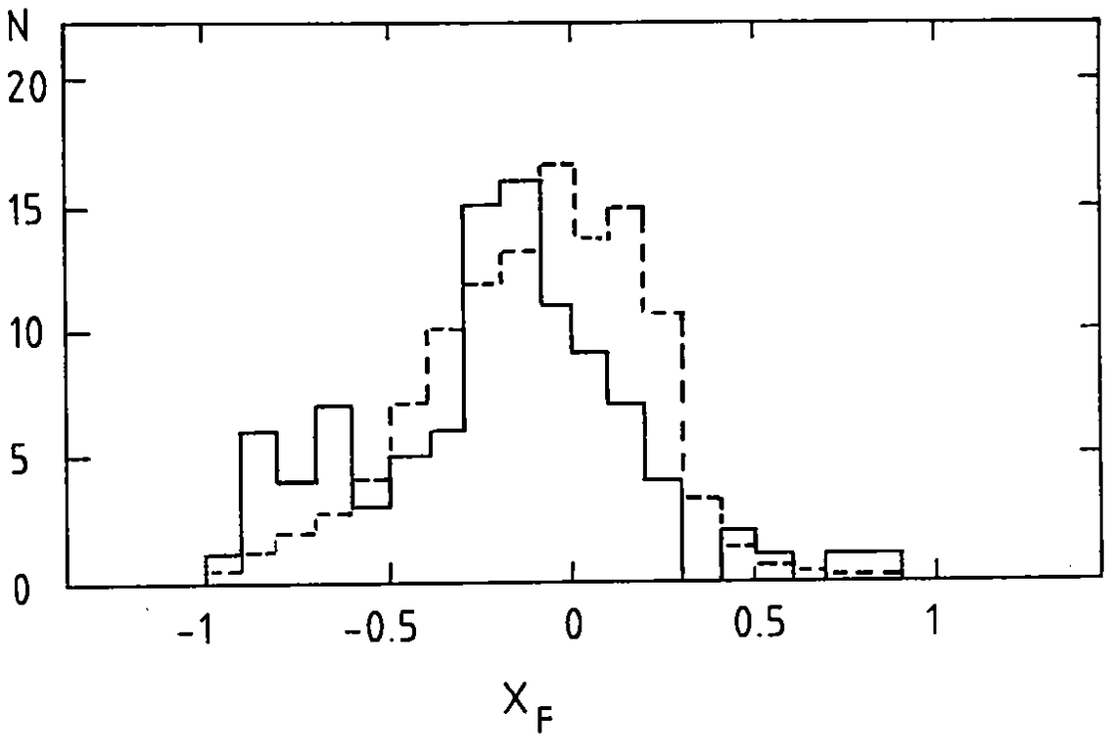

Fig. 9